RESEARCH ARTICLE

Analysis of Fuzzy Logic Controller (FLC) based Hybrid Energy System Fed Microgrid

M.Kondalu[1]* and T.Umamaheswari[2]

[1]Professor, Department of EEE, Malla Reddy Engineering College (Autonomous), Hyderabad, Telangana, India.
[2]Assistant Professor, Department of EEE, Malla Reddy Engineering College (Autonomous), Hyderabad, Telangana, India.

Received: 09 Jan 2023 Revised: 14 Feb 2023 Accepted: 25 Mar 2023

***Address for Correspondence**
M.Kondalu,
Professor,
Department of EEE,
Malla Reddy Engineering College (Autonomous),
Hyderabad, Telangana, India.

ABSTRACT

This paper proposes a fuzzy logic controller (FLC) based hybrid energy system fed microgrid. Generally, most of the researchers consider PI controllers for controlling the proposed system but tuning the gain values of PI is difficult due that getting more errors and adding extra passive elements for compensating frequency fluctuations. In this project, we propose FLC with a model predictive control (MPC) Controlling three-level bidirectional DC/DC converters for grid connections to a HESS in a DC microgrid to begin, a mathematical model of a HESS with a battery and ultra-capacitor (UC) is created, and the neutral point voltage imbalance of a three- level converter is addressed by examining the converter 39;s operating modes. Second, an MPC approach for calculating steady-state reference values in the outer layer and dynamic rolling optimization in the inner layer is proposed for grid-connected converter control. The outside layer guarantees voltage regulation and creates a current predictive model, while the inner layer uses model predictive current control to make the current follow the predicted value, eliminating system current ripple. To realize the high-and low-frequency power allocation for a HESS, this cascaded architecture features two separate controllers and is devoid of filters. As a result, it enables two types of energy storage devices to separately regulate voltage and realizes battery and UC power allocation. Finally, simulation results are designed in MATLAB SIMULINK environment. And obtained results are proof that the proposed system is better than the conventional system.

Keywords: Hybrid energy system; Model predictive control, fuzzy controller.

INTRODUCTION

In order to achieve voltage controller and power apportionment amid battery then UC, this study proposes a two-dimensional MPC approach for grid integration of a HESS's DC/DC translators. The MPC approach suggested in this research has the following primary improvements over the earlier control strategies: 1) The suggested control approach may accomplish quicker DC-link voltage refurbishment then necessary power apportionment among UC and battery when compared to the earlier work in [1]. 2) Filters are not required for the low- and high-frequency power allocations to be realized using this HESS control approach. A high charge/discharge rate in battery contain and avoided with suggested outside voltage stability and gradient regulator. 3) When the program's constant power frequency shifts, the MPC approach performs better dynamically than the PI control technique. This solution has a shorter processing time and a cheaper computing cost when compared to other MPC methods with more complicated models. The PI controller in [2] can command the sensor and UC's charging and disconnecting currents, but it must model the physical network and have access to its governing equations in order to build and fine-tune the control settings. Additionally, the PI control test's function would suffer when the operating point varied and it was unable to preserve optimal controller popular real-time. To provide primary indicator balancing between the cell and UC, Standard [3] suggested an enhanced switching device (EDD) composed of a simulated resistance sag controller and a VCD regulator. However, when the load is regularly replaced, the voltage of the DC MG based on the droop control will oscillate significantly, and voltage drop caused by the reactance will further damage the reliability of a DC link voltage. An algorithm has a significant computational cost and uses a lot of matrices. A wider resonance range is generated by dynamic switching of frequency, necessitating more powerful sorting [4]. A CCS-MPC by the specified duty cycle is what the solution suggested in [6] refers to. The current ripple can be decreased by using a time-varying ratio. Based on the model-predictive PCA determine by a best switch configuration under the assumption of computing the minimal power output error. They also calculate charging and discharging currents of the battery over its entire state of charge. Describes the design of a thrice-level bidirectional DC/DC converter.

DESIGN OF A TEST SYSTEM WITH FIGURES

Topology of the HESS

Fig.1 [7] depicts of a hybrid stowage grid-connected converter's structure. The battery fuels the UC's ability to control its voltage, and the UC uses its thrice-level DC/DC convertor to control of a load demand. On the bus side, those are few different sorts of an input signal standards: full bus voltage (Vdc) and half bus voltage (Vdc/2). The input voltage can be chosen based on the current circumstances. This architecture can successfully lower the battery voltage on each switch and the inductor power ripples, which suppress the higher voltage DC bus power oscillations.

As shown in Fig.1 Vbat and r represent the voltage and resistance values of the battery, respectively; Vuc, ruc, and iuc represent the voltage, resistance, and current of the UC, respectively; L1 and L2 are used to control the battery and the UC's current, while iL1 and iL2 are the equivalent inductor currents. Cuc stands for UC capacitance. The DC bus voltage is Vdc; two similar capacitors, C1 and C2, are represented by their relative voltages, Vc1 and Vc2, as well as by switches SAi I (ranging from 1 to 4), SB1, and SB2 [8].

Battery and UC Mathematical Model

A continuous voltage source and a continuous internal resistor are connected trendy series to make up the battery model. This is how the output voltage is expressed:

$$V_{bat} = E - i_{bat}\gamma \qquad (1)$$

when Ibat is the battery current and E is the potential of the constant voltage source. Due to its high-power density, UC can reduce MG high-frequency power variations [20]. It can decrease the battery's high-power load and increase the battery's lifespan [9]. Aimed at DC-MG schemes, UC cannisterstay easily signifiedthru an ideal series resistor and

capacitor. This straightforward model is capable of capturing a charging and discharging features of UC [22]. The following diagram illustrates the UC's output voltage:

$$V_{uc} = V_c + i_{uc}\gamma_{uc} \quad (2)$$

when Vc is the optimal voltage for a capacitor.

Procedure for NPVB

In reality of a voltage levels those two capacitors of a DC bus side whitethorn vary greatly. It will cause oscillations in neutral point voltage (NPV), sometimes referred to as "middle position stream," which will raise the demand on the reservoir and trigger. To balance Vc1 and Vc2, switching on and off must be done in a balanced manner [19]: When Vdc = 2 Vuc Vdc then the input voltage on the bus side equals the entire DC bus voltage Vdc, capacitors C1 and C2 are connected to the system. Once iL1 > 0, SA1 and SA4 function in buck mode, and when iL1 = 0, SA2 and SA3 operate in boost mode, respectively, neither of which will result in a neutral point current. Only C1 or C2 are connected to the system when Vuc/Vdc = 2, resulting in anNPC. In order to effectively balance Vc1 and Vc2, an NPV balancing technique must be used. The input voltage on the bus cross is currently Vdc=2. The system still functions in buck or boost method, and the capacitors are either charged or discharged, depending on the value of iL1. Whether C1 is connected to the system via SA1 and SA3 or C2 is connected to the system depends on the values of Vc1 and Vc2.Identify whether C2 is connected to the system via SA2 and SA4 versus C1 being connected via SA1 and SA3. The charge controller has two components that work together to regulate the voltage in a UC, bus voltage of the DC MG: if a battery powers in UC, the UC powers the DC bus [9]. Individually component has few control strands: an internal current zone and an outer voltage control plane. Calculating the extrapolative worth of the inductor current required toward stabilize the voltage is the goal of outer voltage stability. The purpose of inner current control is to ensure that the real current follows the extrapolative worth generated by external regulation in order to achieve the goals of outer layer constant forecasted value computation and inner layer dynamic moving utilization.

Control of the outer voltage

For example, battery voltages control. In a change in the UC voltage Vuc container straight affect the variation in current IUC once there is a discrepancy between the rated reference voltage Vuc ref and the UC real voltage Vuc. The convertor arranged the battery lateral runs in boost mode once the battery is exhausted and the UC is charged, and it runs in buck mode when the battery is charged and the UC is discharged. KCL states that the converter's signal is applied in Fig. 2 as iin = iL1-iuc. The below steps can be taken to obtain the current reference, iL2ref:

$$i_{L2\pi ef} = i_{in} \times \frac{V_{uc}}{V_{bat}} \quad (3)$$

The anticipated current, iL2(k + 1), is calculated using both sample voltage and current. This current acts as the reference current for the internal current regulation (iL2ref). Following that, the duty cycle, or dbat, is calculated using the MPCC approach. The schematic for the battery-side control method is shown in Fig. 3.

Create a Battery Gradient Device

The charge is not suitable for frequent charging and draining, so the reaction of the current iL2 should be as gradual as possible. The outside voltage control incorporates a battery current slope limiter that permits a slower changing rate of the estimated current controller, iL2ref. iL2ref (k) and iL2ref(k+1) are characterized as derived for the inductor L2 at the kth and subsequent instants of each sampling time Ts, respectively. The four output of neural network correspond to a fault for every one of the 3 phases and 1 output is ground line. Thus, all outputs is either 0 or 1 suggesting a yes or no fault on the line (A, B, C or G, where A, B and C represents 3 phases of transmission line network and G indicates ground) [1].Therefore, each of different faults be represented accordingly by the various possible permutations. The proposed neural network is able to precisely differentiate ten feasible kind of faults. The table 1 shows the truth value describing faults and efficient operation for each of faults.

SIMULATION AND RESULTS

For creating MPC, the MPC Tool cabinet offers roles, an app, Simulink wedges. The tool cabinet facilitates the proposal of implicit, explicit, adaptive, and gain-scheduled MPCs for linear glitches. You can use single- and multi-stage nonlinear MPC to resolve nonlinear problems. You can use a custom resolution in addition to the deployable optimization solvers that are provided by the toolbox. Run closed-loop simulations in MATLAB and Simulink to assess controller performance shown in the fig 4. Developers can also utilise the principles and features provided to get started with autonomous driving technologies like lane keep assist, path scheduling, path following, and adaptive cruise control straight away.

Step load changes

Fig.4 Only with the suggested MPC approach a bus voltage overshoot stands near 0.8% of a settling period be situated approximately 0.002, the overshoot is approximately 3.5%, along with settling duration remains approximately 0.0025 at 0.4 s through step load. Fig. 4(a) Simulation results using MPC method. (b) Simulation results using PI method. Difference between a PI controller technique and a suggested MPC technique. According to Fig. 4.(b), the bus voltage overshoot with the proposed MPC technique is approximately 0.8%, about settling time is 0.002 s along a step load at 0.2 s; the overshoot approximately 3.5%, the settling duration is approximately 0.0025 s and 0.4 s. Those dynamic performances of a system under the suggested MPC technique is better, as can be observed from the examination of the two methods. The normal operating point of the device will alter, changing the PI controller's ideal settings. As a result, A PI regulator technique can't always preserve optimal controller. To ensure optimum control, the suggested MPC approach can react in real-time in accordance with changes in the state variables.

Change controller parameters

This curve of iL2ref and the subsequent charging and discharging rates of the battery are both directly impacted by the controller parameter i. Fig.4 shows that as I grows from 0.01 A to 0.02 A and finally to 0.05 A, the characteristics of a battery power retort become earlier and quicker. At delta I = 0.05 This device's power level when the actuator is engaged. The variable δi is altered. (c) 0.01, (d) 00.02 and (e) 0.05 As a summary and primary- or secondary-order filters canister remains deleted, the scheme wants to assign high- and low-frequency power variations. To accomplish by same effect of power distribution, a cut-off frequency canister remain modulated indirectly and flexibly thru changing value of the constraints δi.

UC short circuit (SC) fault

The retort of a bus, UC voltages below the suggested MPC approach is seen while taking into account the SC defect of the UC in the HESS. If a UC experiences a SC fault under typical operating conditions on t = 0.3 s, and fault is resolved in 0.05 s. Fig. 5 displays changes to the DC bus , UC voltage (b). According to the simulation results shown in Fig. 5(b), at t = 0.3 s, UC's SC defect causes a sharp drop in both the UC and bus voltages. The issue is fixed within 0.05 seconds. The UC starts to get recharged as the grid's voltage starts to increase. The above figure illustrates that the UC takes a while to attain its initial steady state due to its enormous capacity. The findings demonstrate of scheme meticulous thru suggested MPC technique container immobile be returned to a default functioning mode once the UC short-circuit problem has been repaired.

Photovoltaic Power Fluctuations

This primer is 1000, and at t = 0.5 s and t = 1 s, individually, 100 and 50 DC lots are introduced in corresponding. At time t = 0, the variable PV power is also added. The PV device's power rating is 952 W, and its lowest terminal voltage is 0, as shown in Fig.6. Fig 6 compares the anticipated MPC approach with the PI controller technique and displays the effects of loads and PV power variations on a voltage of a DC bus and UC. According to Fig. 6(a-b), voltage variations in the system meticulous by a PI regulator are higher and voltage constancy is visibly inferior than the system meticulous thru the MPC regulator when t = 1-1.5 s.

(a) The voltage of capacitors C1 and C2. (b) Inductor L1 reference current iL1ref and actual current iL1As can be shown, the thrice-level convertor in Figure. 7's proposed MPC approach can guarantee NPV balance (a). In Fig. 7, low current ripples are obtained, and the real current closely matches the reference current (b).

Comparison with LPF method Stagecapacity change

In a UC and battery reactions to power in the HESS are exposed in Figure 7. The output power of energy storage technologies is limited. The load is connected in 0.4 seconds, and as can be seen in Fig.7 (a) and (b), the UC responds right away to offer instantaneous power recompense while battery output influence grows gradually toward provide steady-state power. Power sags are lessened by the energy storage devices working together. Both strategies, as shown in Fig.8 (a) and (b), can reduce the number of battery cycles when there are significant high-frequency power fluctuations during the first couple of seconds. It will enhance the pressure of the UC and make it more capable of bearing energy at low frequencies. Overall, the two strategies can produce the same control performance. The suggested approach without LPF optimizes the operational state of the energy storage device and simplifies the controller architecture.

CONCLUSION

Under this Paper recommend an MG-fed FLC-based hybrid energy system. The majority of researchers typically think about using PI controllers to control the proposed systems, but fine-tuning the gain values of these controllers is challenging because they produce more error and require more passive components to compensate for frequency changes. In this paper suggest using FLC with an MPC to operate thrice-level simultaneous DC/DC translators in a DC MG for grid integration with a HESS. After a two-stage enhancing architecture, a battery container prevents larger voltage level variations in a similar grid voltage level. Unlike the control scheme, the MPC controller does not require a time-consuming phase of parameter modifications in order to account for many random variables at every sampling interval. The MPC method, which is based on a constant switching frequency, also achieves rapid and accurate voltage and current regulation with reduced ripple. Eventually, the control scheme is simplified while battery performance is extended, and power fluctuations may be distributed without the need for filters.

REFERENCES

1. D. Liang, C. Y. Qin, S. Y. Wang, and H. M. Guo,"Reliability evaluation of DC Distribution power network," in Proceedings of 2018 China International Conference on Electricity Distribution,Tianjin, 2018, pp. 654–658.
2. Z. Huang, J. Ma, J. Zeng et al., "Research status and prospect of control and protection technology for DC distribution network," in Proceedings of 2014 China International Conference on Electricity Distribution, Shenzhen, Sep. 2014, pp. 1488–1493.
3. K. A. Joshi and N. M. Pindoriya, "Case-specificity and its implications in distribution network analysis with increasing penetration of photovoltaic generation," CSEE Journal of Power and Energy Systems, vol. 3, no. 1, pp. 101–113, Mar. 2017.
4. Y. Xu, T. Y. Zhao, S. Q. Zhao, J. H. Zhang, and Y. Wang, "Multiobjective chance-constrained optimal day-ahead scheduling considering BESS degradation," CSEE Journal of Power and Energy Systems, vol. 4, no. 3, pp. 316–325, Sep. 2018.
5. Y. Sun, Z. Zhao, M. Yang, D. Jia, W. Pei and B. Xu, "Overview of energy storage in renewable energy power fluctuation mitigation,"CSEE Journal of Power and Energy Systems, vol. 6, no. 1, pp.160–173, Mar. 2020.
6. U. Manandhar, N. R. Tummuru, S. K. Kollimalla, A. Ukil, G. H.Beng, and K. Chaudhari, "Validation of faster joint control strategy for battery and supercapacitor-based energy storage system," IEEE Transactions on Industrial Electronics, vol. 65, no. 4, pp. 3286–3295,Apr. 2018.
7. H. J. Wang and J. C. Zhang, "Research on charging/discharging control strategy of battery-super capacitor hybrid energy storage system in photovoltaic system," in Proceedings of the 2016 IEEE 8thInternational Power Electronics and Motion Control Conference,Hefei, 2016, pp. 2694–2698.

8. U. Manandhar, B. F. Wang, X. N. Zhang, G. H. Beng, Y. T. Liu, andA. Ukil, "Joint control of three-level DC-DC converter interfacedhybrid energy storage system in DC microgrids," IEEE Transactions on Energy Conversion, vol. 34, no. 4, pp. 2248–2257, Dec. 2019.
9. J. Cao and A. Emadi, "A new battery/ultracapacitor hybrid energy storage system for electric, hybrid, and plug-in hybrid electric vehicles," IEEE Transactions on Power Electronics, vol. 27, no. 1, pp.122–132, Jan. 2012.
10. Q. W. Xu, X. L. Hu, P. Wang, J. F. Xiao, P. F. Tu, C. Y. Wen, and M.Y. Lee, "A decentralized dynamic power-sharing strategy for hybridenergy storage system in autonomous DC microgrid," IEEETransactions on Industrial Electronics, vol. 64, no. 7, pp. 5930–5941,

Table.1:Values of Various Faults

Fault Types	Phase A	Phase B	Phase C	Ground
AG	1	0	0	1
BG	0	1	0	1
CG	0	0	1	1
AB	1	1	0	0
BC	0	1	1	0
CA	1	0	1	0
ABC	1	1	1	0
No Fault	0	0	0	0

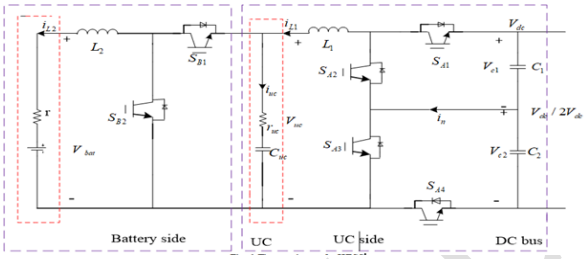

Fig .1. The topology of HESS

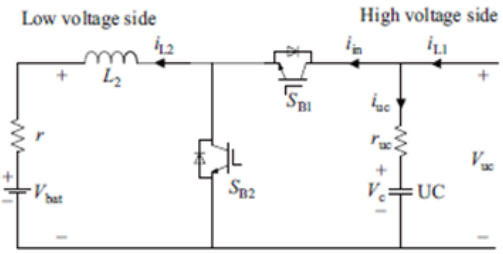

Fig.2. Topology of battery

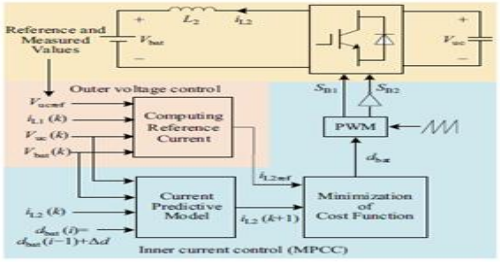

Fig.3. Battery control block schematic

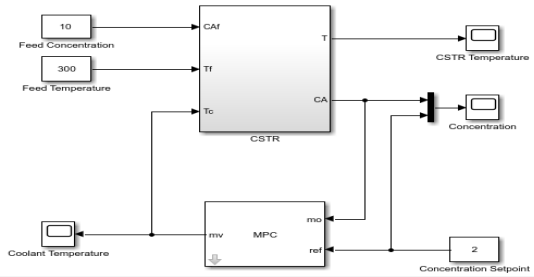

Fig .4 Schematic Simulink diagram

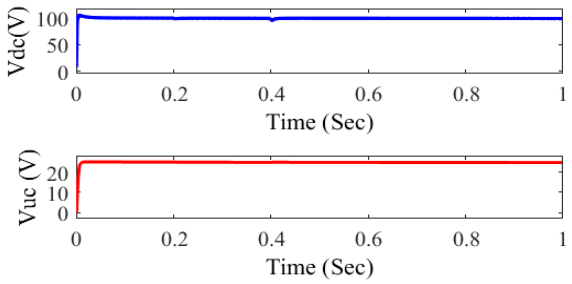

(a)

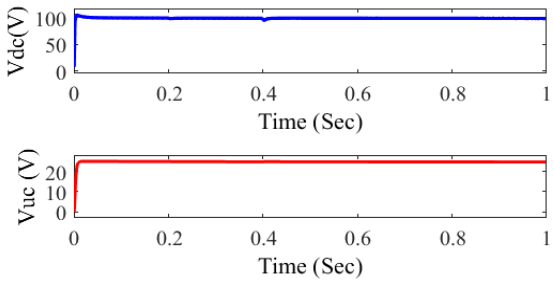

(b)

Fig. 4(a) Simulation results using MPC method. (b) Simulation results using PI method.

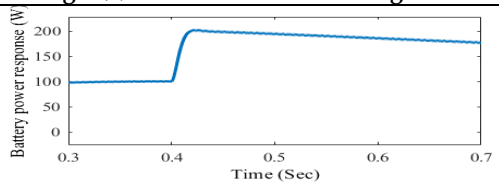

(c)

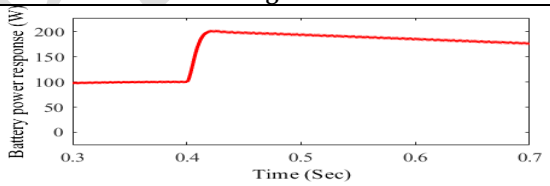

(d)

At delta I = 0.05 | **At delta I =0.02**

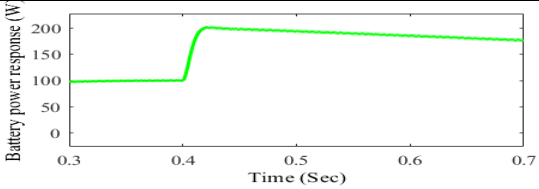

(e)

At delta I = 0.01

Fig. 5. This device's power level when the actuator is engaged. The variable δi is altered. (c) 0.01, (d) 00.02 and (e) 0.05

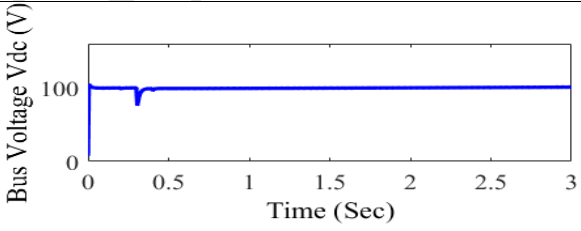

Fig. 5.(a) SC of UC in case of voltage response.

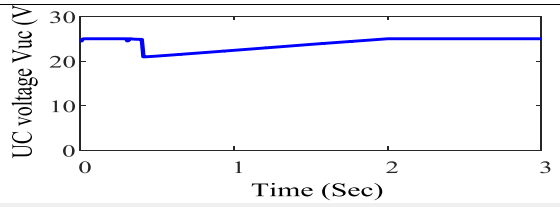

Fig. 5.(b) UC voltage

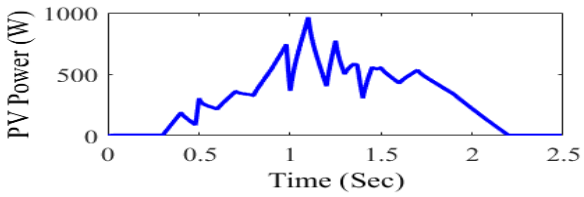

Fig. 6. PV module output power

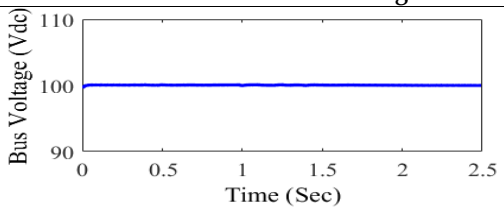

(a) Bus voltage

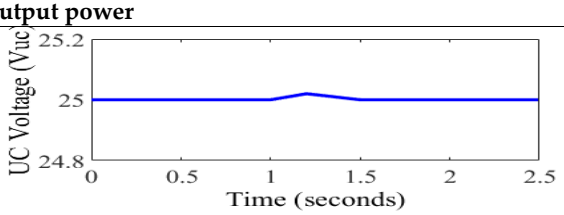

(b) UC voltage

Fig.7 Using MPC controller (a) Bus voltage, (b) UC voltage

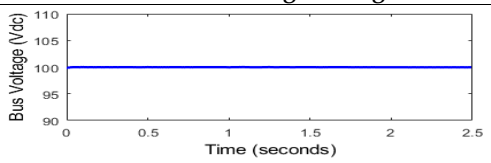

(a)

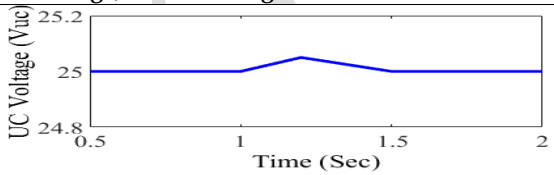

(b)

Fig. 8 (b) demonstrates that the highest voltage fluctuation with the MPC controller is 0.02 V, while by the PI Regulator, it is 0.05 V.

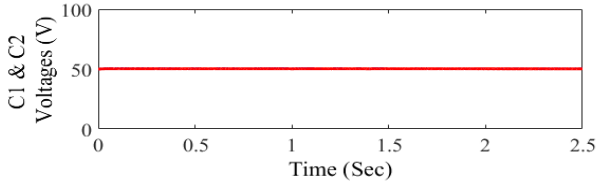

(a)

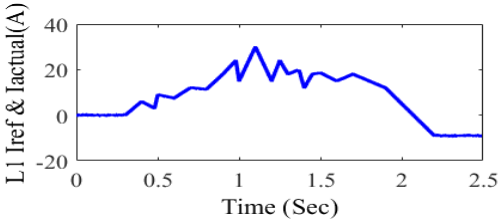

(b)

Fig. 9 The efficiency of the suggested MPC technique

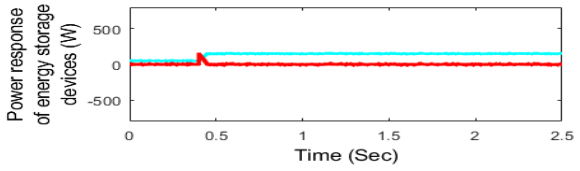

(a) Without LPF

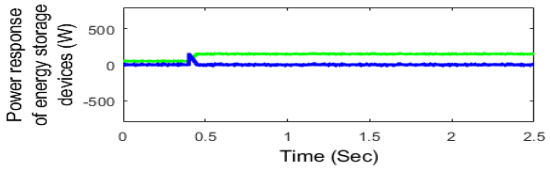

(b) With LPF

Fig 10. Photo voltaic power fluctuations.

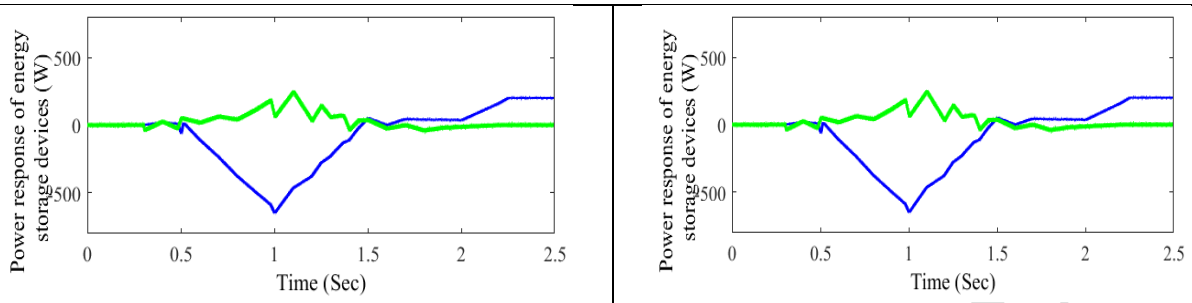

(a) Without LPF (b) With LPF

Fig. 11. Control distribution of the HESS